BJRS
BRAZILIAN JOURNAL OF RADIATION SCIENCES

doi.org/10.15392/2319-0612.2024.2674
2024, 12(4B) | 01-21 | e2674
Submitted: 2024-08-29
Accepted: 2025-04-07

Thermohydraulic Performance in SMR Reactors with Mixed Oxide (U, Th)O2 Fuel: A Computational Approach

Santos[a*], P. E. M.; Betancourt[a], M. C.; Mazaira[a], L. Y. R.; García Hernández[b], C. R.; Dominguez[c], D. S.; Lira[d], C. A. B. O.

[a]Universidade Federal de Pernambuco – UFPE
[b]Instituto Superior de Tecnologías y Ciencias Aplicadas – InSTEC
[c]Universidade Estadual de Santa Cruz – UESC
[d]Centro Regional de Ciências Nucleares do Nordeste - CRCN-NE

*Correspondence: pedro.emanuel@ufpe.br

Abstract: This paper presents a computational study on the thermohydraulic performance of subchannels within Small Modular Reactor (SMR) configurations using Mixed Oxide (MOX) fuels comprising (U, Th)O_2 alongside subchannels containing conventional UO_2. The research aims to evaluate these fuel types operational efficiency and safety within the context of small-scale reactors. Utilizing a Computational Fluid Dynamics (CFD) model implemented in OpenFOAM, this study considers the variability of the thermophysical properties of the materials as influenced by temperature changes. The findings reveal that MOX fuels exhibit lower maximum temperatures than UO_2, suggesting a more uniform radial temperature distribution. Moreover, both the cladding and coolant temperatures remain within safe operational limits across all scenarios examined, highlighting the potential of MOX fuels to enhance the safety and efficiency of SMRs. This analysis advances our understanding of the thermal behavior of advanced fuel compositions in nuclear reactors. It underscores the importance of comprehensive thermohydraulic studies in the design and operation of next-generation nuclear power systems.

Keywords: CFD, SMR, MOX.

SBPR

BJRS
BRAZILIAN JOURNAL OF RADIATION SCIENCES

doi.org/10.15392/2319-0612.2024.2674
2024, 12(4B) | 01-21 | e2674
Submitted: 2024-08-29
Accepted: 2025-04-07

Desempenho Termohidráulico em Reatores SMR com Combustível de Óxido Misto (U, Th)O2: Uma Abordagem Computacional

Resumo: Este artigo apresenta um estudo computacional sobre o desempenho termohidráulico de subcanais em configurações de Reatores Modulares Pequenos (SMR) usando combustíveis de Óxido Misto (MOX) compostos por (U, Th)O_2, ao lado de subcanais contendo UO_2 convencional. A pesquisa tem como objetivo avaliar a eficiência operacional e a segurança desses tipos de combustível no contexto de reatores de pequena escala. Utilizando um modelo de Dinâmica dos Fluidos Computacional (CFD) implementado no OpenFOAM, este estudo considera a variabilidade das propriedades termofísicas dos materiais conforme influenciadas pelas mudanças de temperatura. Os resultados revelam que os combustíveis MOX apresentam temperaturas máximas mais baixas do que o UO_2, sugerindo uma distribuição de temperatura radial mais uniforme. Além disso, tanto as temperaturas do revestimento quanto do refrigerante permanecem dentro dos limites operacionais seguros em todos os cenários examinados, destacando o potencial dos combustíveis MOX para aumentar a segurança e a eficiência dos SMRs. Esta análise avança nossa compreensão do comportamento térmico de composições de combustível avançadas em reatores nucleares e ressalta a importância de estudos termohidráulicos abrangentes no design e operação de sistemas de energia nuclear de próxima geração.

Palavras-chave: CFD, SMR, MOX.

SBPR

1. INTRODUCTION

The search for sustainable energy solutions has motivated interest in small modular reactors (SMRs) due to their versatility, reduced costs, and possible deployment in remote locations [1]. Safety and efficiency are crucial in nuclear reactors, and mixed oxide (MOX) fuels, such as those composed of thorium (Th) and uranium (U) oxides, emerge as promising alternatives to conventional uranium oxide (UO_2). This is due to reduced natural uranium consumption and decreased high-level nuclear waste [2,3].

The adoption of MOX in SMRs can enhance the sustainability of the nuclear fuel cycle and assist in managing plutonium inventories [2]. However, the thermohydraulic behavior of these systems in small-scale reactors requires detailed studies. Thermohydraulic analysis is essential to assess the suitability of the design and the reactor's responsiveness under various conditions.

In this work it was condicted a comparativea analysis was performed between the thermohydraulic performance of MOX and UO_2 fuels in SMRs, using thermohydraulic simulation models developed in the OpenFOAM software. The core temperature distribution, maximum fuel temperatures, cladding, and coolant temperatures were evaluated. The study aimed to assess the technical feasibility of MOX in SMRs.

Emphasis was placed on the analysis of an integral pressurized water modular reactor with Uranium-Thorium oxide (U-Th MOX) fuel mixtures. The main objective was to develop a computational model capable of calculating the most important thermohydraulic parameters in the section where the highest power is produced in the core. Using the developed model, temperature and power profiles were determined in the hottest channel, as well as temperature profiles in the cladding and water.

2. MATERIALS AND METHODS

This section describes the reactor's characteristics, the developed geometry and mesh, and the computational tools used. It also presents the values of the model parameters and a detailed description of the materials properties, allowing for a comprehensive and accurate analysis of the system's behavior.

2.1. Characteristics of the mPower Reactor Core

The core design will be based on the Small Modular Reactor (SMR) characteristics from BWX Technologies/Bechtel Generation mPower, which has a nominal power of 180 MWe per module. The mPower core consists of 69 fuel assemblies, standard supplied by Westinghouse Company, arranged in a square structure with a spacing of 21.5 cm between them. Each fuel assembly consists of 264 fuel rods, 24 guide tubes for the control rods, and a central rod for instrumentation [4]. Figure 1 provides important details about the characteristics and dimensions of the fuel rods and guide tubes used in the reactor. With this supplementary visual information, it is possible to have a more complete and accurate understanding of the structure and operation of the system.

Figure 1: Specifications and Measurements of Fuel Rods and Guide Tubes.

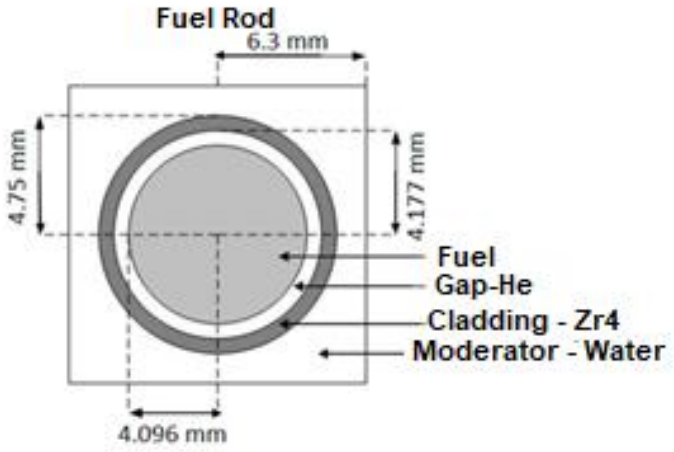

Source: Adapted from Stefani [5].

In [5], an evaluation was conducted on the feasibility of various recycling alternatives for thorium and uranium, as well as plutonium, as options for use as fertile isotopes in the core of an integral pressurized water reactor (iPWR). The standard uranium fuel cycle with enrichment below 5% was used as a parameter. For the application of MOX (U, Th)O_2 mixtures, a partially loaded core with MOX fuel was considered to ensure an extended 48-month cycle. Twenty-four fuel assemblies, corresponding to one-third of the core, were loaded with MOX fuel, while the remainder contained UO_2 fuel, as illustrated in Figure 2.

Figure 2: MOX Fuel Distribution in the Core.

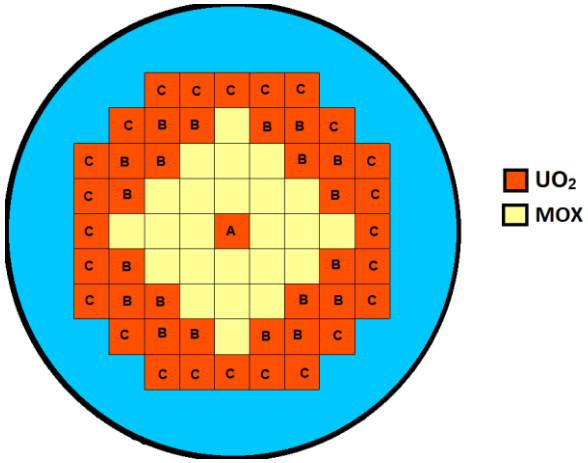

Source: Authors.

As shown in Table 1, thorium is used in a mixture with uranium, in a ratio of 6.97% uranium to 93.03% thorium.

Table 1 : Composition in % by mass of MOX fuel assemblies

MOX (U, Th)O_2	**%**
U 232	0.31
U 233	49.79
U 234	29.63
U 235	7.21
U 236	12.97
U 238	0.09
Total U	6.97
Total Th	93.03

This modular reactor project features a unique and distinct characteristic, as the coolant used does not require a dissolved absorber to assist in reactivity control. Moreover, the extended fuel cycle lasts 48 months, considered a single-step fuel cycle where all fuel assemblies are replaced after four years. It is important to emphasize that there was no need for refuelling or exchanging fuel assemblies during the cycle period for the neutronic calculations performed. These details are crucial for a more complete and accurate analysis of the operation and performance of this particular modular reactor.

2.2. Neutronic Calculations

The distribution of power density across the different types of fuels analyzed is essential for conducting the thermohydraulic simulation. Power distribution information is necessary to calculate the maximum power value in the core for both MOX (Th, U)O_2 fuel assemblies and UO_2 assemblies. The results obtained from the neutronic calculations are presented in Figure 4, allowing for a more precise and reliable analysis of the power distribution in the reactor core [6].

For the fuel assembly channel with UO_2, the distribution is adjusted by Equation 1, while for the channel with MOX (Th, U)O_2 fuel, the distribution is adjusted by Equation 2, where "x" represents the height of the fuel rod, measured in meters. These equations are essential for obtaining the proper power distribution in the different channels of the reactor core, allowing for a more detailed and precise analysis of the thermohydraulic behavior of the system.

$$P\left[\frac{W}{m^3}\right] = 7{,}1 * 10^7 * x^6 - 5 * 10^8 * x^5 + 1{,}39 * 10^9 * x^4 - 1{,}97 * 10^9 * x^3 + 1{,}12 * 10^9 * x^2 + 3{,}12 * 10^8 * x + 1{,}05 * 10^8 \quad [1]$$

$$P\left[\frac{W}{m^3}\right] = 6{,}24 * 10^7 * x^6 - 4{,}41 * 10^8 * x^5 + 1{,}22 * 10^9 * x^4 - 1{,}7 * 10^9 * x^3 + 9{,}5 * 10^8 * x^2 + 2{,}53 * 10^8 * x + 8{,}12 * 10^7 \quad [2]$$

Figure 3: Power density distribution for UO_2 and (Th, U)O_2 in a core with MOX (Th, U)O_2

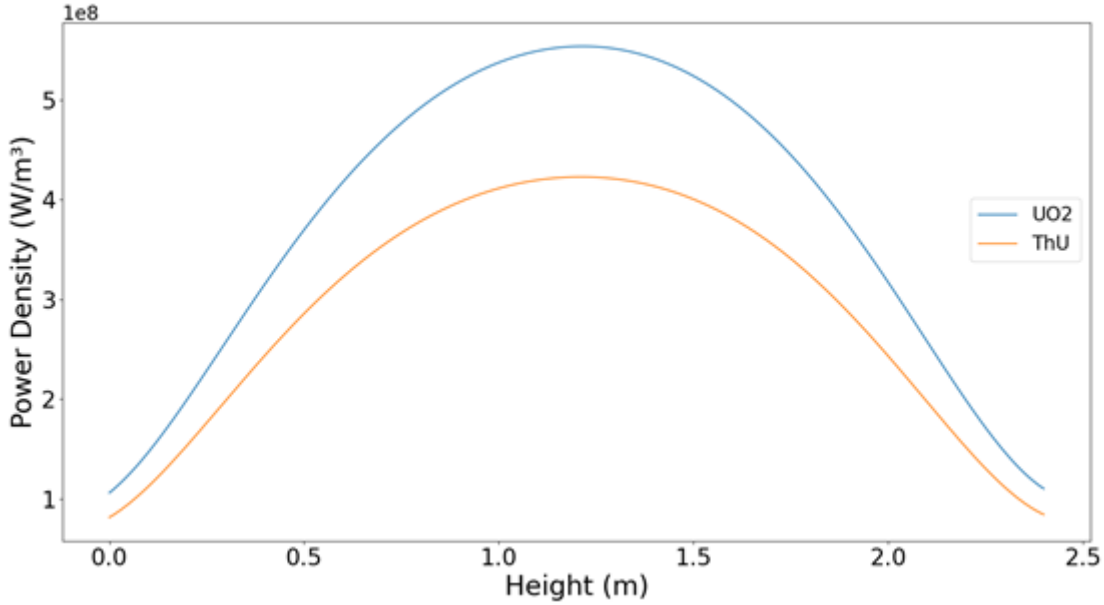

Source: Authors.

It is worth noting that all the calculations presented consider the beginning of the cycle (BOC - Beginning of Cycle) for the fuel assemblies in question. This consideration is crucial for a more accurate and reliable analysis of the system's thermohydraulic behavior, ensuring the use of the most up-to-date and precise information about the combustion process in the reactor core. As a result, the findings obtained from the equations presented are even more relevant for evaluating the performance of the modular reactor under study.

2.3. Computational Model for Thermohydraulic Calculation

One of the thermohydraulic constraints related to the fuel is that the temperature reached cannot exceed its melting point. The maximum temperature in the fuel depends primarily on the thermal conductivity and the linear power density in the rods. The pressure of the coolant in the reactor is controlled by an electrically heated pressurizer located above the steam generator, ensuring stable operation and maintaining pressure under all operating conditions. The coolant's temperature in the reactor must be kept below the saturation point to prevent boiling in the core. The power density of the designed reactor core is

approximately 65 kW/liter, significantly lower than the power density of a larger pressurized water reactor (PWR) [7]. Table 2 displays the main thermohydraulic parameters used in the model for conducting the thermohydraulic analysis of the hottest part of the core.

Table 2: Thermohydraulic Parameters

Parameter	Value
Thermal Power	530 MW
Pressure	14.8 Mpa
Inlet Temperature	290 °C
Outlet Temperature	318.8 °C
Mass Flow Rate in the Core	3345 Kg/s

Computational Fluid Dynamics (CFD) techniques have proven to be a reliable option for anticipating thermohydraulic performance in nuclear reactors. A notable aspect of CFD simulations is the methodology employed in describing physical processes, as it uses a spatial distribution of these processes, enabling the identification of local phenomena crucial for the design and safety of nuclear reactors [8]. The thermohydraulic calculations for this study were conducted using the OpenFOAM software.

OpenFOAM (Open source Field Operation And Manipulation) is a free and open-source numerical simulation toolkit that allows users to modify or develop solvers for specific engineering issues, broadening its applicability. Primarily employed in computational fluid dynamics to solve problems related to the mechanics of continuous media, it offers a wide range of algorithms to handle typical CFD numerical challenges. Thanks to its extensive library, it can address everything from complex flows and heat transfer to acoustics, solid mechanics, and electromagnetism. OpenFOAM also provides utilities to assist in pre- and post-processing data and meshes. In OpenFOAM, the user defines the solver to be used for solving partial differential equations and the settings for parameters, boundary conditions, geometry, and mesh [9,10,11]. In this study, the solver chtMultiRegionSimpleFoam was employed, which meets the project requirements.

2.4. Geometry and Spatial Discretization

Examining the critical fuel assembly where maximum power is generated is crucial to ensure that the fuel meets thermal constraints. To optimize computational resources and simplify calculations, symmetry conditions were employed to model the highest power subchannel in the fuel assembly. The dimensions of the subchannel, presented in Figure 1, have an active length of 240 cm. The Design Modeler of the Ansys software was used to create the necessary geometry for this research. Figure 4 displays the geometry developed for this study.

Figure 4: Top and Isometric view of the fuel channel geometry.

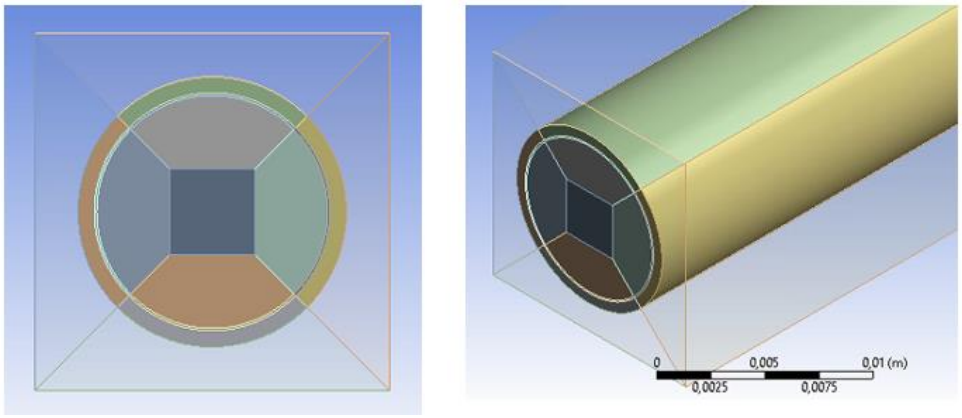

Source : Authors.

The geometry and the precision required for the solution determine the mesh configuration and the number of elements used in the spatial discretization. This study employed a structured mesh to adapt to the channel geometry. The geometry was divided into several parts to generate a more structured mesh and optimize the computational resources used.

Mesh refinement was conducted in areas near the walls to ensure that velocity and temperature gradients were resolved accurately. To verify the solution, a mesh independence study was carried out with various configurations. It was found that a mesh with 3,876,000 elements and 4,202,801 nodes provides a mesh-independent solution. Figure 5 shows the cross-sectional view of the subchannel. The mesh was generated using the multi-zone

method, which involves intertwining independent zones, allowing for the automatic decomposition of the geometry into swept and free regions.

Figure 5: Mesh used in the discretization of the domain.

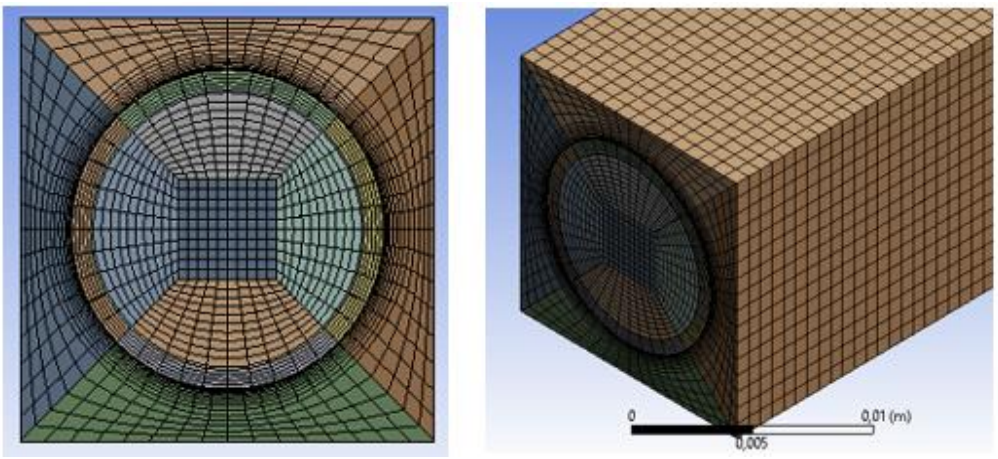

Source : Authors.

When evaluating the mesh's quality, indicators such as Skewness, Aspect Ratio, and Orthogonal Quality are considered. The Skewness parameter measures how close a face or cell is to the ideal, equilateral or equiangular, with 0 representing the ideal value and 1 the worst possible value. In this study, the maximum value obtained was 0.5. The Aspect Ratio parameter corresponds to the ratio between the length of the longest edge and the length of the shortest edge, where an ideal value is equal to 1; in this work, the maximum value found was 28.66. This value represents a theoretical ideal, achievable only in a perfect bidimensional mesh. In the case of OpenFOAM, it is recommended that this value be less than 100 [12,13].

The primary parameter evaluated, Orthogonal Quality, involves the angle between the vector connecting two mesh nodes (or control volume) and the normal vector relative to each integration point surface (n) associated with that edge. For this parameter, 1 is considered an optimal value and 0 is a poor value, resulting in a minimum value of 0.632 in this study. The mesh used in the modelling meets the established quality criteria, ensuring the reliability of the results obtained. The parameters for evaluating the quality of the mesh are presented in Table 3 [12,13].

Table 3: Thermohydraulic Parameters

Parameter	Value			
	Minimum	**Average**	**Maximum**	**Ideal**
Orthogonal Quality	0.63214	0.95615	1	1
Aspect Ratio	1.2383	8.4952	28.66	1
Skewness	1.31E-10	0.13533	0.5	0

2.5. Thermophysical Properties of UO_2

The density as a function of temperature can be calculated using Equation 3 [14]:

$$\rho(T)\left[{}^{kg}/_{m^3}\right] = \rho(273)\frac{L(273)^3}{L(T)} \quad [3]$$

Where $\rho(273)$ is the density at 273 K; L(273) and L(T) are the lengths at 273 K and at temperature T (K), respectively. The ratio of the length at 273 K to the length at temperature T (K) can be calculated using Martin's equations for the thermal expansion of solid UO_2, given by Equation 4 and Equation 5, for the ranges 73 ≤ T < 923 K and 923 ≤ T ≤ 3120 K, respectively [14]:

$$\frac{L(T)}{L(273)} = 0.99734 + 9.802 \cdot 10^{-6}T - 2.705 \cdot 10^{-10}T^2 + 4.291 \cdot 10^{-13}T^3 \quad [4]$$

$$\frac{L(T)}{L(273)} = 0.99672 + 1.179 \cdot 10^{-5}T - 2.429 \cdot 10^{-9}T^2 + 1.219 \cdot 10^{-12}T^3 \quad [5]$$

The recommended correlation for specific heat (Cp) is given by Equation 6 for the range 298.15 K ≤ T ≤ 3120 K, where τ is the temperature in K divided by 1000 [14]:

$$C_p = 52.1743 + 87.951\tau - 84.2411\tau^2 + 31.5421\tau^4 - 2.6334\tau^4 - 0.7139\tau^{-2} \quad [6]$$

The recommended correlation for thermal conductivity (λ), considering 95% of the theoretical density, is given by Equation 7, where τ is the temperature in K divided by 1000 [14]:

$$\lambda_{95}\left[{}^{W}/_{m\,K}\right] = \frac{100}{7.5408+17.692t+3.6142t^2} + \frac{6400}{t^{5/2}}e^{-\frac{16.35}{t}} \quad [7]$$

2.6. Thermophysical Properties of (U, Th)O_2

The recommended equation for the theoretical density of (U, Th)O_2 as a function of UO_2 content (x) and temperature (298–1600 K) is given by Equation 8 [15]:

$$\rho_{th} = 10.087 - 2.891 \cdot 10^{-4}T - 6.354 \cdot 10^{-7}xT + 9.279 \cdot 10^{-3}x + 5.111 \cdot 10^{-6}x^2 \quad [8]$$

Equation 9 was derived for the heat capacity of the mixed oxide ($U_{(1-y)}$, Th_y)O_2 [15]:

$$C_p \left[J/_{mol\ K}\right] = y(55.9620 + 0.05126T - 3.6802 \cdot 10^{-5}T^2 + 9.2245 \cdot 10^{-9}T^3 - 5.74031 \cdot 10^5 T^{-2}) + (1-y)(52.1743 + 0.08795T - 8.4241 \cdot 10^{-5}T^2 + 3.1542 \cdot 10^{-8}T^3 - 2.633 \cdot 10^{-12}T^4 - 7.1391 \cdot 10^5 T^{-2}) \quad [9]$$

Equation 10 for the thermal conductivity (λ) of (U_y, $Th_{(1-y)}$)O_2 with 95% of the theoretical density as a function of composition (y) and temperature (T) is valid from 873 to 1873K [15]:

$$\lambda_{95}(W/mK) = \frac{1}{-0.0464 + 0.0034y + (2.5185 \cdot 10^{-4} + 1.0733 \cdot 10^{-7}y)T} \quad [10]$$

2.7. Flow and Boundary Conditions

In this work, single-phase water is employed as the coolant to simulate the typical conditions of a pressurized water reactor subchannel. The mass flow rate for the subchannel is set to 0.18 kg/s, derived from the total core mass flow rate of 3345 kg/s. This value is adjusted proportionally to the cross-sectional area of the fluid in the subchannel relative to the total cross-sectional fluid area within the reactor core. At the inlet, we use the OpenFOAM *flowRateInletVelocity* boundary condition, specifying a temperature of 563.15 K and a pressure of 14.8 MPa, consistent with the reactor's operating parameters.

For the solid walls (fuel cladding surface), a *no-slip* (noSlip) condition is applied, implying zero coolant velocity adjacent to the walls. Heat transfer between the cladding and

the fluid is modeled by the *compressible::turbulentTemperatureCoupledBaffleMixed* boundary condition, ensuring proper coupling of temperature and turbulence parameters across the solid-fluid interface.

To optimize computational resources while preserving accuracy, symmetry planes are introduced where the geometry permits such simplification, allowing the simulation of only a representative portion of the domain without compromising the quality of the results. Turbulence is treated using the standard k-ε model, which provides a balanced combination of numerical fidelity and moderate computational cost, making it well-suited for nuclear subchannel analyses [16].

3. RESULTS AND DISCUSSIONS

The thermohydraulic study of the subchannels was conducted using the axial power density distributions obtained by the SERPENT code, which are later fitted to Equations 1 and 2. The beginning of the cycle (BOC) was considered for the fuel, meaning new fuel, without considering the use of burnable poisons. Figure 7 presents the axial temperature of the water at the contact point with the cladding wall for both subchannels. The maximum recorded temperature is 608.8 K for MOX (U, Th)O_2 and 618.04 K for UO_2, as shown in Figure 6. In the case of UO_2, the temperature is higher than the saturation temperature (614.23 K) for the coolant pressure.

Figure 6: Axial Water Temperature Distribution for UO_2 and $(Th,U)O_2$.

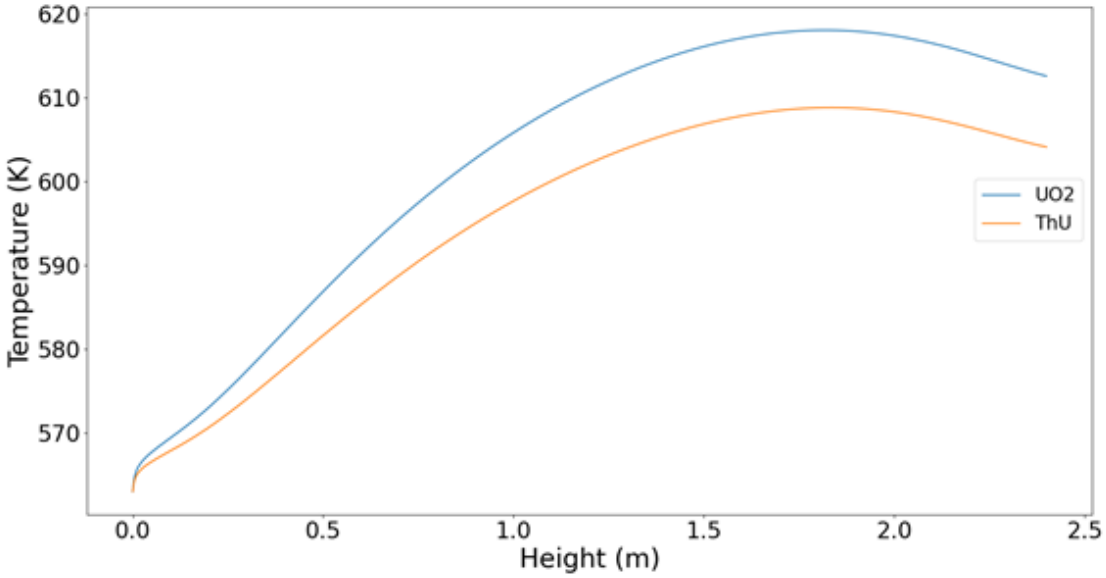

Source : Authors.

The axial temperature distribution at the center of the water, that is, between two fuel rods at a distance of 0.0063 m from the center of the fuel, is shown in the main water volume region. Figure 7 displays the axial temperature distribution at the center of the water along the height of the subchannel containing UO_2, reaching a maximum temperature of 608.68 K, below the water's saturation temperature.

In Figure 8, the axial temperature distribution at the center of the water is presented along the height for the subchannel with $(Th,U)O_2$, where the maximum temperature reached was 600.8 K.

In the case of the assemblies with UO_2, the maximum cladding temperature reached 667.85 K, while for the assemblies with $(Th,U)O_2$, the maximum temperature was 647.9 K. In both cases, the cladding temperatures were well below the 1477.59 K limit reported in accident scenarios [17].

Figure 7: Axial Water Temperature Distribution at the Center for UO_2 in a Core with MOX $(Th,U)O_2$.

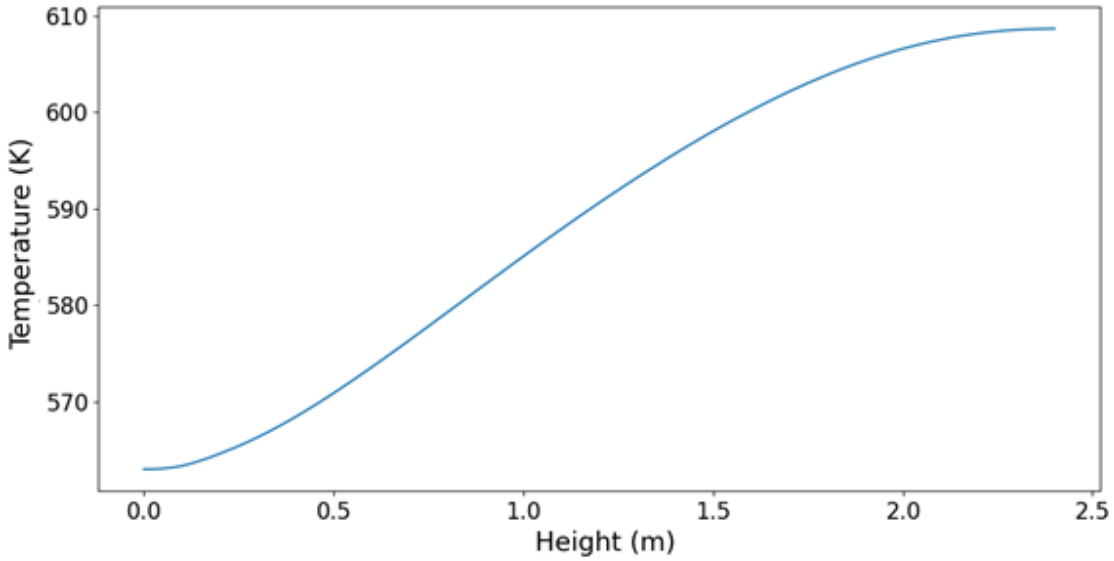

Source : Authors.

Figure 8: Axial Water Temperature Distribution at the Center for MOX $(Th,U)O_2$.

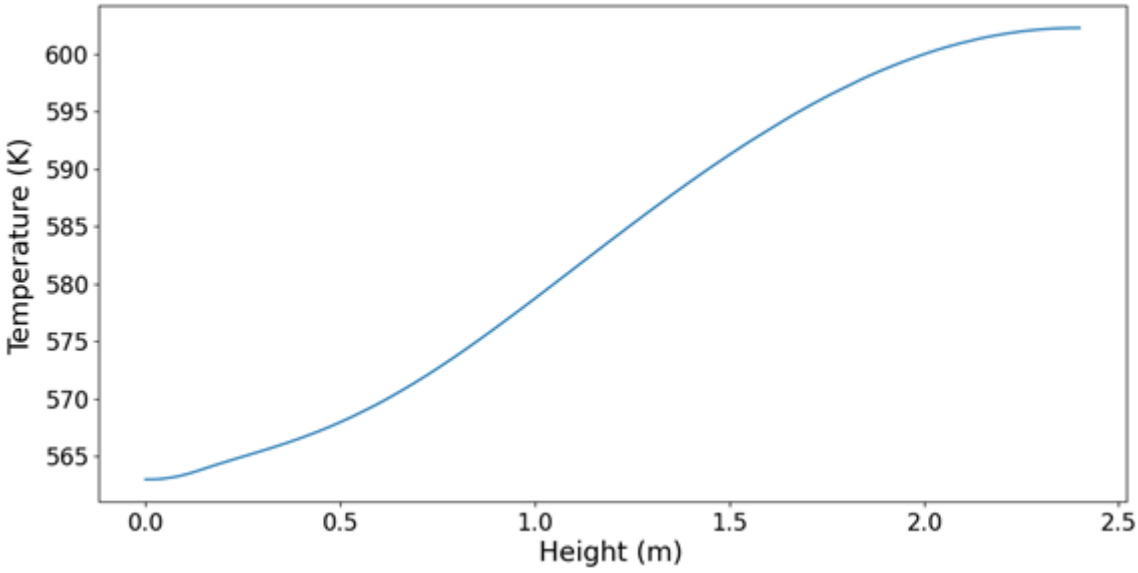

Source : Authors.

The axial temperature distribution in the fuel is displayed, passing through the point of maximum temperature, which is located at the center of the fuel element. In the subchannel with UO_2, the maximum temperature reached was 1842.71 K, considerably below the 3120 K melting point. In contrast, in the subchannel with $(Th,U)O_2$, the maximum

temperature reached was 1281.6 K, well below the 3220 K melting point of (Th,U)O_2. The fuel temperature increases as it progresses through the subchannel, up to approximately halfway, following the fuel's power distribution. The difference between the temperature distributions for the highest power subchannels in the assemblies loaded with UO_2 and (Th,U)O_2 is illustrated in Figure 9, showing a difference of 561.11 K between the maximum fuel temperatures.

Figure 9: Axial Fuel Temperature Distribution for UO_2 and (Th,U)O_2.

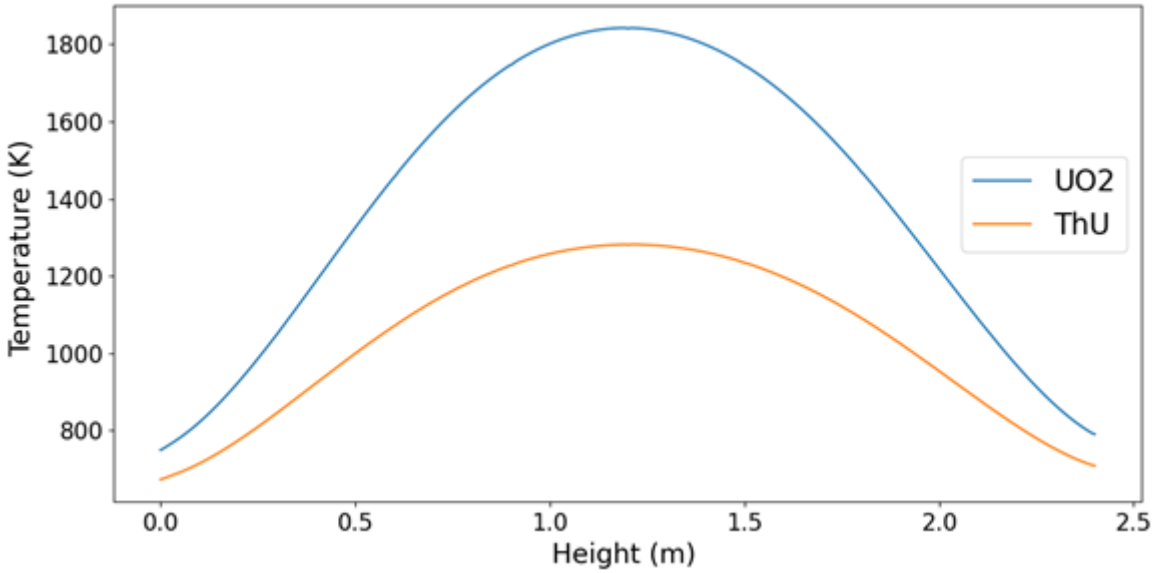

Source : Authors.

The radial temperature distribution in the subchannel is displayed, passing through the point of maximum temperature in the fuel, from the center of the fuel to the coolant. It can be observed that the temperature varies between the different materials that make up the subchannel, regardless of the type of fuel used. When comparing the distributions, it is noted that, even with a significant difference in the maximum temperature at the center of the fuels, this difference decreases as it approaches the helium, resulting in a small difference in the coolant temperature. Figure 10 illustrates the difference between the radial temperature distributions for the highest power subchannels in the assemblies loaded with UO_2 and (Th,U)O_2.

Figure 10: Radial Temperature Distribution for UO_2 and $(Th,U)O_2$.

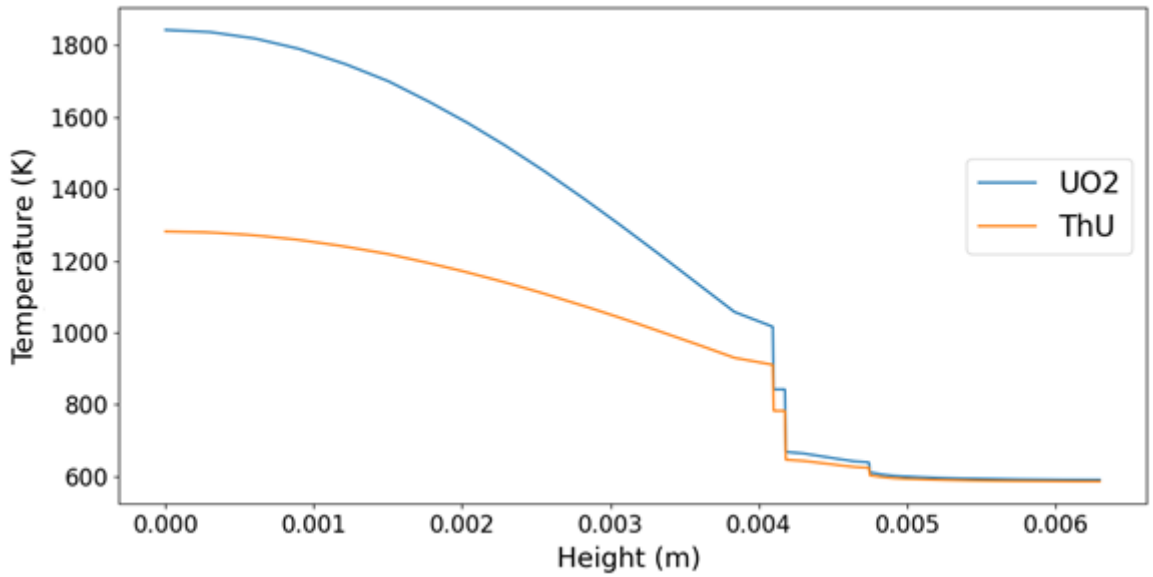

Source : Authors.

The main results obtained from the thermohydraulic analysis of the subchannels for both fuel types are summarized in Table 4. These values correspond to the beginning of cycle (BOC) conditions and provide insight into the thermal behavior of the system.

Table 4: Thermohydraulic Parameters

Parameter	UO_2	$(Th,U)O_2$
Maximum water temperature at the clad wall (K)	618.04	608.8
Maximum water temperature at the center of the subchannel (K)	608.68	600.8
Maximum clad temperature (K)	667.85	647.9
Maximum fuel temperature (K)	1842.71	1281.6

Source : Authors.

4. CONCLUSIONS

In this study, a three-dimensional subchannel model was developed and implemented, considering the thermophysical properties of materials as a function of temperature, using CFD code to evaluate the thermohydraulic behavior of an SMR reactor based on its critical fuel assembly with a mixture of uranium and thorium oxides (U, Th)O_2. The axial power distribution was obtained in the reactor's critical subchannel and in the subchannel that generates the highest power of the MOX fuel, using the Serpent code for neutronic calculation and expressions of the thermophysical properties of the materials available in the literature.

The analysis of the coolant revealed that the maximum coolant temperature in the critical subchannels with UO_2 and (Th,U)O_2 was 618.04 K and 608.8 K, respectively, values close to the saturation temperature under reactor conditions. Additionally, the water temperatures in the centers of the subchannels remained below the saturation temperature, meeting the reactor design requirement that the bulk temperature of the coolant fluid remains below this temperature to prevent boiling in the core.

The axial temperature distribution in the fuel elements was evaluated, revealing the temperature behavior along the fuel rods and their respective maximum temperatures. The analysis of the radial temperature distribution allowed for observing the impact of different fuel materials on the radial temperature.

The temperature distributions in the subchannels were calculated, indicating that the MOX fuel reaches a maximum temperature of 1281.6 K, while the UO_2 fuel reaches 1842.71 K. Additionally, the maximum cladding temperatures for the MOX (U, Th)O_2 and UO_2 fuels were 647.9 K and 667.85 K, respectively, which are satisfactory when compared to the 1477.59 K limit for accident scenarios. Thus, the study contributes to a better understanding the thermohydraulic behavior in SMR reactors with different fuel types.

ACKNOWLEDGMENT

The authors thank CNEN (Comissão Nacional de Energia Nuclear) and FACEPE (Fundação de Amparo à Ciência e Tecnologia de Pernambuco).

FUNDING

The authors would like to thank the CNEN scholarship (Request 01351.000104/2022)

CONFLICT OF INTEREST

All authors declare that they have no conflicts of interest.

REFERENCES

[1] INGERSOLL, D., T. Deliberately small reactors and the second nuclear era. **Progress in Nuclear Energy**, v. 51, n. 4-5, p. 589-603, 2009.

[2] CHEN, B.; YU, N.; FU, L.; ZHU, Y.; VAN REE, T.; WU, Y. Mixed oxides in nuclear fuels. *In*: Elsevier (Ed). **Metal Oxides in Energy Technologies**. Cambridge, MA, US: Elsevier Inc., 2019. p. 73–89. ISBN 978-0-12-811167-3.

[3] IAEA. Potential of thorium based fuel cycles to constrain plutonium and reduce long lived waste toxicity. **IAEA-TECDOC-1349**, International Atomic Energy Agency, Vienna, 2003.

[4] CARELLI, M. D.; INGERSOLL, D. T. **Handbook of Small Modular Nuclear Reactors**, Cambridge, MA, US: Elsevier Inc., 2015. p. 1–516. ISBN 978-0-85709-853-5.

[5] STEFANI, G. L.; MAIORINO, J. R.; MOREIRA, J. M. L.; SANTOS, T. A.; ROSSI, P. C. R. Feasibility to convert an advanced PWR from UO2 to a mixed (U,Th)O2 core.

PROCEEDINGS OF THE INTERNATIONAL NUCLEAR ATLANTIC CONFERENCE 2017, Belo Horizonte, Brazil. **Anais**...International Nuclear Atlantic Conference, 2017.

[6] BETANCOURT, M. C.; GARCÍA HERNÁNDEZ, C. R.; DOMINGUEZ, D. S.; ROJAS MAZAIRA, L. Y.; BRAYNER, C. A.; ROSALES GARCÍA, J. A.; IGLESIAS, S. M. Mixed-oxide fuel strategies in an integral pressurized water reactor. **Progress in Nuclear Energy**, v. 139, 103844, 2021.

[7] ERIGHIN, M. A. A 48-month extended fuel cycle for the B&W mPowerTM small modular nuclear reactor. **International Conference on the Physics of Reactors 2012, PHYSOR 2012: Advances in Reactor Physics**. v.2, p. 1315-1330, 2012.

[8] WANG, M.; WANG, Y.; TIAN, W.; QIU, S.; SU, G. H. Recent progress of CFD applications in PWR thermal hydraulics study and future directions. **Annals of Nuclear Energy**. v.150, 107836, 2021.

[9] JASAK, H. OpenFOAM: Open source CFD in research and industry. **International Journal of Naval Architecture and Ocean Engineering**. v. 1, n. 2, p. 89–94, 2009.

[10] JASAK, H.; JEMCOV, A.; TUKOVIC, Z. OpenFOAM : A C ++ Library for Complex Physics Simulations. **International Workshop on Coupled Methods in Numerical Dynamics**. p. 1–20, 2007.

[11] OpenFOAM. OpenFOAM: Programmers Guide v1812. Available at: https://foam.sourceforge.net/docs/Guides-a4/ProgrammersGuide.pdf. Accessed on: 17 Apr. 2023.

[12] GULLBERG, R. Computational fluid dynamics in OpenFOAM. Mesh Generation and Quality. **TKP**, v. 4555, 2017.

[13] FABRITIUS, B., TABOR, G. Improving the quality of finite volume meshes through genetic optimisation. **Engineering with Computers**, v.32, 425–440, 2016.

[14] IAEA. Thermophysical Properties of Materials for Nuclear Engineering: A Tutorial and Collection of Data. **IAEA-THPH**, International Atomic Energy Agency, Vienna, 2008.

[15] IAEA. Thermophysical Properties Database of Materials for Light Water Reactors and Heavy Water Reactors. **IAEA-TECDOC-1496**, International Atomic Energy Agency, Vienna, 2006.

[16] MOUKALLED, F.; MANGANI L.; DARWISH M. The finite volume method in computational fluid dynamics. **Fluid Mechanics and Its Applications**. v. 113, 2016.

[17] HACHE, G.; CHUNG, H. M. The History of LOCA Embrittlement Criteria. PROCEEDINGS OF THE TWENTY-EIGHTH WATER REACTOR SAFETY INFORMATION MEETING 2001, Bethesda, MD, United States. **Anais**… 28th Water Reactor Safety Information Meeting, 2001.

LICENSE